

MODELLING THE ISOTOPE ENRICHMENT OF LEAF WATER

B. BARNES[†], G. FARQUHAR[†], AND K. GAN[†]

ABSTRACT. Farquhar and Gan [8] have proposed a model for the spatial variation in the isotopic enrichment of H_2^{18}O across a leaf, which is specifically formulated for monocotyledoneous leaves. The model is based on the interaction between mass fluxes longitudinally within the xylem, and fluxes laterally through veinlets into the lamina mesophyll, where moisture leaves the leaf through transpiration. The lighter, more abundant, molecule H_2^{16}O escapes preferentially with the evaporating water, resulting in the enrichment of H_2^{18}O at these sites. Enriched water diffuses throughout the leaf, and it is this spatial distribution of enriched water which the model seeks to capture. In this paper we present a general formulation of the model in terms of mass flux, extending it to include variable transpiration rates across the leaf surface, as well as a tapering xylem. Solutions are developed for the general case and, since the solutions present in the form of Kummer functions, properties are established as well as methods for estimating the solutions under certain conditions relevant to the biology. The model output is compared with Gan's data ([10], [11]) collected from maize plants.

Keywords: leaf water modelling, oxygen isotope ratio, enrichment.

1. INTRODUCTION AND MOTIVATION

The isotopic distribution of leaf water can provide valuable information concerning the interactions between plants and the environment. Oxygen atoms within leaf water molecules, may be ^{16}O or ^{18}O : 99.8% of the oxygen isotopes are ^{16}O , but there is a small percentage of the heavier isotope ^{18}O . As water transpires from the leaves, the lighter isotope escapes preferentially, facilitating the enrichment of H_2^{18}O within the leaf. The isotope ratio of the enriched leaf water is encoded within the organic matter of the plant, and since the isotopes interact with atmospheric gases, this ratio effects the isotopic composition of atmospheric CO_2 .

Ramifications of this leaf enrichment are broad. Following from the isotopic exchange between leaf water and atmospheric CO_2 , the ratio of ^{18}O to ^{16}O in atmospheric CO_2 provides a means of assessing GPP (gross primary production) [6]. Also, the isotopic variation of atmospheric oxygen can determine the balance between terrestrial and marine net productivity over millennial time scales. This can be established from a record of the oxygen isotope ratio in gas extracted from ice cores. Cellulose encodes humidity and the isotopic composition of source water, from which temperatures and climate can be reconstructed, and thus previous climatic conditions can be established. And further, these isotopic compositions have been correlated with yield potential in cereal crops, where differences in yield potential arise through genetic differences. (For a full discussion of the significance and ramifications of this enrichment, see [8].)

In order to inform such applications a number of models, developed for analogous applications, have been adapted to describe the enrichment of leaf water: the Craig-Gordon model [4] [5], a two-pool model [9], a Péclet model [7] and a string-of-lakes model [12]. For an extensive review of these models see [11]. However, none of

these models fully explain the observed features of spatial enrichment within the leaf [11].

The Farquhar-Gan model [8] is a recently proposed model developed to address previous shortcomings. It is specifically a model pertaining to monocotyledoneous leaves, where the configuration and leaf transport system have been highly simplified. The model describes the spatial variation of enriched water resulting from advective and diffusive fluxes, operating both longitudinally in the xylem and laterally into the lamina mesophyll, within the leaf.

In this paper we provide a succinct mathematical formulation of the Farquhar-Gan model for the general case of variable transpiration rates along the leaf length. We describe two distinct methods of solution, and extend the particular solution presented in [8] to the general case. Since the solution presents in the form of special functions (hypergeometric Kummer functions) we include methods for estimating the solution in particular cases, as well as in general. Further, we present mathematically derived properties, which agree with proposed quantities in [8]. We also extend the formulation to include tapering xylem. In specific cases an analytic solution could be attained; however, in the general case numerical methods provided a means of establishing how the results of this formulation differed from those for which the xylem was assumed cylindrical.

In Sections 2 and 3, we formulate the model and non-dimensionalise the equation. Section 4 establishes the solution to this equation, and then we examine some of its properties in Section 5, and interpret them in a biological context in Section 6. As evaluating the solution is not straightforward without mathematical software, this is followed by a section on calculating and estimating the solution (Section 7). We adapt the formulation to that for tapering xylem in Section 8, and present numerical solutions for comparison with the non-tapering case. Finally, Section 9 provides a comparison between the model predictions and data measurements, and an appraisal of the model.

2. MODEL FORMULATION

A model for the concentration of isotopes within a leaf is constructed by considering the mass fluxes into, and from, the xylem. For any small section of the xylem ‘cylinder’ there is mass flux into a section due to forward advection with the flow of water along the leaf, as well as diffusion (longitudinally). Mass also flows laterally from the xylem into the lamina mesophyll tissue to the sites of evaporation, and is lost through transpiration. Diffusion operates laterally as well. Our formulation models the variation of the isotopic concentration in the xylem fluid, with changing length l along the vein, assuming that the system is in steady state with respect to time.

We model the xylem as a cylinder of cross-sectional area $a_x = a_x(l)$ and length l_m , with $l = 0$ at the leaf base where water flows into the cylinder, and $l = l_m$ at the tip. (A modification for the case of tapering xylem is given in Section 8.) Consider a section of the xylem ‘cylinder’, from l to $(l + \Delta l)$, as illustrated in Figure 1, where motion is taken as positive in the direction of increasing l . The model is formulated by establishing the mass flux through this section of the lighter, abundant H_2^{16}O , and then modified to describe the enrichment of the heavier H_2^{18}O molecules.

2.1. Mass balance. The rate of change in mass within this section is equal to the difference between the mass entering and the mass leaving. Let M be the bulk molar mass of the lighter molecule H_2^{16}O in a section of unit length. Let $J(l, t)$ be the molar mass flux of H_2^{16}O (at l , per unit of area, per unit of time) through the section. The mass loss from the section, per unit of time, via transpiration is $Es\Delta l$,

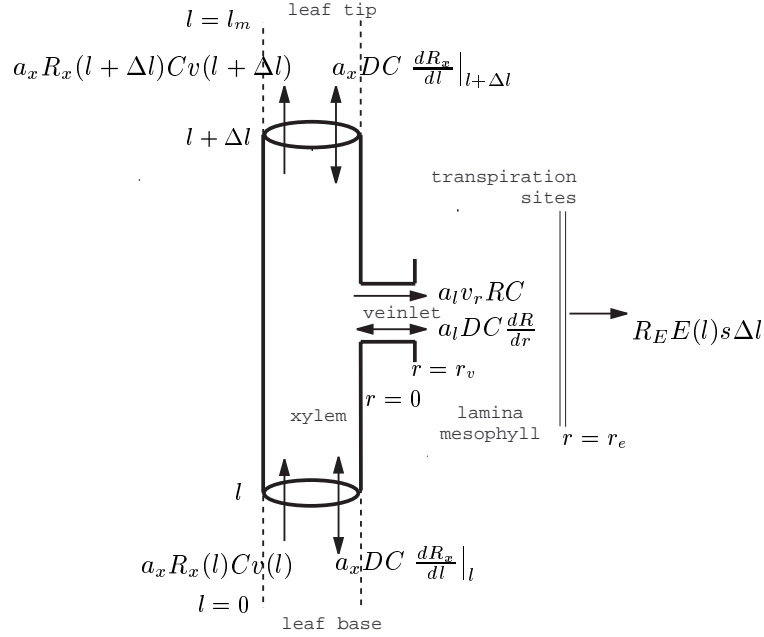


FIGURE 1. Diagrammatic representation of fluxes in a section of the xylem, which lead to equation (3) for the longitudinal fluxes in the xylem, and equation (7) for the fluxes into the lamina mesophyll.

where $E = E(l)$ is the rate of transpiration of H_2^{16}O at l , and s the distance from the xylem over which it acts (equivalent to the interveinal spacing).

Thus, the rate of change in the molar mass of H_2^{16}O in the section can be expressed as,

$$\frac{\partial(M\Delta l)}{\partial t} = [J(l, t)a_x(l) - J(l + \Delta l, t)a_x(l + \Delta l)] - E(l)s\Delta l.$$

Since the system is at steady state with respect to time, the rate of change in mass (the LHS) is zero and the expression can be considered a function of l alone. Dividing by Δl , and taking the limit as $\Delta l \rightarrow 0$, leads to

$$(1) \quad \frac{d(Ja_x)}{dl} = -Es.$$

That is, the total mass flux of H_2^{16}O is balanced by its loss through transpiration. However, we are interested in the enrichment of the heavier H_2^{18}O molecules within the leaf, and thus incorporate this aspect into the formulation below.

2.2. Longitudinal advective and diffusive fluxes in the xylem. The flux J is comprised of two parts: $J = C_{16}v(l) - D\frac{dC_{16}}{dl}$. The former, an advective flux with the bulk water flow $C_{16}v(l)$, where C_{16} is the molar mass of H_2^{16}O per unit of volume and $v(l)$ is the velocity of the bulk flow at l , and the latter, a diffusive flux assumed to operate longitudinally (one dimensional diffusion). To formulate the model for the heavier isotopes, we assume that the diffusion constant D is the same for H_2^{18}O and H_2^{16}O . (There may be slight differences between the diffusivities; however, any such difference is very small compared with D , see [14].) Note that the molar mass of water has $C = C_{18} + C_{16}$, where C_{18} is the concentration of the heavy H_2^{18}O molecules and C_{16} (as above) is that of the significantly more abundant

and lighter H_2^{16}O . While C_{18} and C_{16} may vary, C remains constant with time. Define $R_x = C_{18}/C_{16}$ and then, in terms of R_x ,

$$C_{18} = \frac{CR_x}{1 + R_x} \quad \text{and} \quad C_{16} = \frac{C}{1 + R_x}.$$

From above, applying these expressions for C_{18} and C_{16} , and with R_J the relative proportion of heavy molecules with respect to the flux J ,

$$\begin{aligned} R_J J &= \frac{C_{18}}{C_{16}} C_{16} v - D \frac{d}{dl} \left(\frac{C_{18}}{C_{16}} C_{16} \right) \\ &= \frac{R_x C v}{1 + R_x} - D \frac{d}{dl} \left(\frac{C R_x}{1 + R_x} \right) \\ &= \frac{R_x C v}{1 + R_x} - \frac{DC}{(1 + R_x)^2} \frac{dR_x}{dl}. \end{aligned}$$

Since the abundance of the heavier H_2^{18}O is close to 0.2%, compared with the 99.8% of H_2^{16}O , then $R_x \ll 1$ so that $C_{16} \approx C$ and the mass flux of the heavy isotope can be expressed as,

$$R_J J \approx R_x C v - DC \frac{dR_x}{dl}.$$

From here forward we will assume equality to hold in the place of these approximations, since we have shown there to be negligible effect on accuracy.

For the mass loss of the heavier isotope in transpiring water, let R_E denote the ratio of the heavy isotope to the lighter one in evaporating water. Thus the molar mass loss of the heavy isotope from the section, per unit of time, through transpiration is $R_E E s \Delta l$.

Equation (1) for the flux of the heavy isotope, becomes

$$(2) \quad \frac{d(R_J J a_x)}{dl} = -R_E E s.$$

Thus,

$$\begin{aligned} \frac{d(R_J J a_x)}{dl} &= \frac{d(R_x C v a_x)}{dl} - \frac{d \left(D \frac{d(R_x C)}{dl} a_x \right)}{dl} = -R_E E s \\ \Rightarrow \frac{d(R_x C v a_x)}{dl} &= a_x D \frac{d^2(R_x C)}{dl^2} + D \frac{d(R_x C)}{dl} \frac{da_x}{dl} - R_E E s. \end{aligned}$$

Expanding these derivatives, and in the case of ‘cylindrical’ xylem so that $da_x/dl = 0$ (the case of tapering xylem is dealt with in Section 8),

$$(3) \quad C v a_x \frac{dR_x}{dl} + R_x \frac{d(C v a_x)}{dl} = a_x D \frac{d^2(R_x C)}{dl^2} - R_E E s,$$

Note that v , R_x and E are all functions of l (distance along the leaf).

Now Cv is the bulk flow (per unit of area) through the xylem, equivalent to the flow of H_2^{16}O (as discussed above), and can be equated with the water loss through transpiration via

$$(4) \quad C v(l) a_x = \int_0^{l_m} E s dl - \int_0^l E s dl \stackrel{\text{def}}{=} I_m - I.$$

Thus I is the water loss (of H_2^{16}O) through transpiration from the leaf base to l along the leaf, and I_m is the transpiration loss along the full length. It follows that

$$(5) \quad \frac{d(C v a_x)}{dl} = -\frac{dI}{dl} = -E(l)s.$$

Substituting these equations back into equation (3), rearranging, and noting that C is constant,

$$(6) \quad a_x DC \frac{d^2 R_x}{dl^2} - (I_m - I) \frac{dR_x}{dl} + (R_x - R_E) \frac{dI}{dl} = 0.$$

2.3. Advection and diffusion into the lamina. Advection and diffusion fluxes into the lamina, in a direction perpendicular to the longitudinal fluxes considered above (see Figure 1), are included in the model through a replacement expression for $(R_x - R_E)$. Following Figure 1, for a fixed value of l along the leaf, let R denote the isotope ratio (abundance of H_2^{18}O to H_2^{16}O) in water at some point between R_x (at the xylem) and R_e (at the evaporation site), and consider the variation of R with distance r from the xylem in a direction perpendicular to it. Advection into the lamina at r , with velocity v_r (assumed constant along r), can be expressed as $a_l RC v_r$, where a_l is the area through which the process operates and $C \approx C_{16}$ is assumed a good approximation as discussed in Section 2.2. The opposing diffusion is proportional to the gradient in the isotope ratio along r , and is expressed as $-a_l D d(RC)/dr$. Thus,

$$(7) \quad a_l v_r R_E C = a_l v_r RC - a_l D \frac{d(RC)}{dr} \quad \text{or} \quad v_r R_E = v_r R - D \frac{dR}{dr}.$$

Integrating over the distance r (perpendicular to the xylem) $r = 0$ at the xylem to $r = r_R$ (where the isotope ratio is R), and denoting $R = R_e$ as the local isotope ratio at the sites of evaporation, we can solve this equation to give

$$(8) \quad R = R_E + (R_x - R_E) e^{v_r r / D},$$

$$(9) \quad R_e = R_E + (R_x - R_E) e^{v_r r_e / D} = R_E + (R_x - R_E) e^{P_r}.$$

Equation (8) is the general solution, and equation (9) is the particular solution used to characterise the system, with $r = r_e$ the effective length from the xylem (at l) to the transpiration sites. P_r is defined as the Péclet number, and is a measure of the relative significance of the advective and diffusive processes acting perpendicular to the xylem into the lamina.

In order to obtain a second expression for $R = R_e$ we include some further system relationships (see [8]). The transpiration rate E is related to the leaf-to-air humidity difference by

$$(10) \quad E = g(w_i - w_a),$$

where g is the conductance to diffusion of water vapour through the boundary layer and stomata, and w_i and w_a are the internal (at the evaporation sites) and external (ambient) humidities, respectively. Further, the local isotope ratio at the sites of evaporation, R_e , is related to that of the transpiring water, R_E , via

$$(11) \quad R_E E = \frac{g}{\alpha_k} \left(\frac{R_e}{\alpha^+} w_i - R_v w_a \right),$$

where α_k is the overall fractionation associated with diffusion, α^+ is the depression of vapour pressure of the heavier isotope, and R_v is the isotope ratio of water vapour. Now dividing equation (11) by equation (10) and rearranging the terms, we obtain a second expression for R_e ,

$$(12) \quad R_e = \alpha^+ \alpha_k (1 - h) R_E + \alpha^+ h R_v.$$

We note here that, along the pathway of evaporative enrichment, the isotope ratios at the sites of evaporation and the evaporative flux could become equal at some maximum value $R_M = R_e = R_E$. From equation (12), with $R_M = R_e = R_E$

$$(13) \quad R_M = \frac{\alpha^+ h R_v}{1 - \alpha^+ \alpha_k (1 - h)}.$$

Equating the two expressions for R_e , equations (9) and (12), and including equation (13),

$$\begin{aligned} R_E &= \frac{\alpha^+ h R_v - R_x e^{P_r}}{1 - e^{P_r} - \alpha^+ \alpha_k (1 - h)} \\ (14) \quad &= \left(\frac{R_x e^{P_r}}{h'} - R_M \right) k, \end{aligned}$$

where

$$h' = 1 - \alpha^+ \alpha_k (1 - h) \quad \text{and} \quad k = \frac{h'}{e^{P_r} - h'}.$$

Using equation (14), we can now derive an expression for $(R_x - R_E)$ which includes the effect of diffusion between the lamina and the xylem:

$$\begin{aligned} R_x - R_E &= R_x - k \left(\frac{R_x e^{P_r}}{h'} - R_M \right) \\ &= k R_M - \left(k \frac{e^{P_r}}{h'} - 1 \right) R_x \\ &= k R_M - \left(\frac{h'}{e^{P_r} - h'} \frac{e^{P_r}}{h'} - 1 \right) R_x \\ (15) \quad &= k(R_M - R_x). \end{aligned}$$

Note that the effect of the Péclet number P_r is included through k .

2.4. The model equation. Substituting equation (15) into the differential equation (6) our model becomes

$$(16) \quad a_x CD \frac{d^2 R_x}{dl^2} - (I_m - I) \frac{dR_x}{dl} + k(R_M - R_x) \frac{dI}{dl} = 0.$$

2.5. Boundary conditions. At the tip of the leaf, where $l = l_m$, we consider a xylem section without the fluxes at $l + \Delta l$:

$$a_x R_x C v(l_m) - a_x DC \frac{dR_x}{dl} - R_E E s \Delta l = 0.$$

But $v(l_m) = 0$, and as $\Delta l \rightarrow 0$ we obtain one boundary condition

$$(17) \quad \frac{dR_x}{dl} = 0.$$

The second condition is obtained similarly, by considering the xylem section at the base of the leaf where $l = 0$:

$$a_x R_x C v(0) - a_x DC \frac{dR_x}{dl} - R_E E s \Delta l = 0.$$

In this case $v(0) \neq 0$, and as $\Delta l \rightarrow 0$

$$(18) \quad R_x(0) = \frac{D}{v(0)} \left. \frac{dR_x}{dl} \right|_{l=0}.$$

3. SCALING THE EQUATION

Dividing equation (16) by I_m (where I_m is the water loss through transpiration from definition (4)),

$$0 = \frac{a_x CD}{I_m} \frac{d^2 R_x}{dl^2} - \left(1 - \frac{I}{I_m} \right) \frac{dR_x}{dl} + k(R_M - R_x) \frac{d(I/I_m)}{dl}.$$

Now set $f = 1 - I/I_m$, noting that f is a monotonically increasing function ranging from 0 to 1, which denotes the fraction of water not yet transpired. (Note, when E does not vary with l (length along the leaf), then $f = 1 - l/l_m$ from definition (4).)

Including f in the above expression, and since $v(0) = I_m/(a_x C)$ is the velocity in the xylem at the leaf base,

$$\begin{aligned} 0 &= \frac{D}{v(0)} \frac{d^2 R_x}{dl^2} - f \frac{dR_x}{dl} + k(R_M - R_x) \left(-\frac{df}{dl} \right) \\ &= \frac{D}{v(0)l_m^2} \frac{d^2 R_x}{d(l/l_m)^2} - \frac{f}{l_m} \frac{dR_x}{d(l/l_m)} + \frac{k(R_M - R_x)}{l_m} \left(-\frac{df}{d(l/l_m)} \right). \end{aligned}$$

We now apply a change of variable: $x = 1 - l/l_m$ and $y = (\Delta_M - \Delta_x)/\Delta_M$, where $\Delta_x = R_x/R_s - 1$ (and $\Delta_M = R_M/R_s - 1$) with R_s the isotope ratio of source water. Thus x is a measure of distance along the leaf, with $x = 1$ at the base and $x = 0$ at the tip. We define Δ_x as the isotopic composition in xylem water (Δ_M as the maximum such composition), and thus y is a proportional measure of the distance of Δ_x from a maximum value Δ_M , and $y \in [0, 1]$. The Péclet number relates the advective flux to the diffusive flux through the ratio (velocity \times distance)/ D . Setting $P = v(0)l_m/D$, where P is the Péclet number for the longitudinal fluxes in the xylem, leads to a simpler form of the equation:

$$\begin{aligned} 0 &= \frac{1}{P} \frac{d^2 R_x}{dx^2} + f \frac{dR_x}{dx} + k(R_M - R_x) \frac{df}{dx} \\ &= -\frac{1}{P} \frac{d^2 y}{dx^2} - f \frac{dy}{dx} + ky \frac{df}{dx} \\ &= \frac{d^2 y}{dx^2} + Pf \frac{dy}{dx} - kPy \frac{df}{dx}. \end{aligned}$$

The boundary conditions require the same variable transformation. Noting that at $l = l_m$ we have $x = 0$, the first condition (equation (17)) transforms to

$$\frac{dy}{dx} = 0 \quad \text{at} \quad x = 0.$$

For the second condition (equation (18)), at $l = 0$ we have $x = 1$. In terms of the new variables x and y ,

$$\begin{aligned} 0 &= R_x(0) - \frac{1}{P} \frac{dR_x}{d(l/l_m)} \Big|_{l=0} \\ &= R_M - y(1)R_M - \frac{1}{P} R_M \frac{dy}{dx} \Big|_{x=1} \\ &= 1 - y(1) - \frac{1}{P} \frac{dy}{dx} \Big|_{x=1}. \end{aligned}$$

Thus, for independent variable x (where x is a measure of distance along the leaf, $x = 1 - l/l_m$) and dependent variable y (a measure of the isotope ratio, $y = 1 - \Delta_x/\Delta_M$), both dimensionless and defined over the unit interval $[0, 1]$, and $f = f(x)$ (the fraction of water not yet transpired), the model is

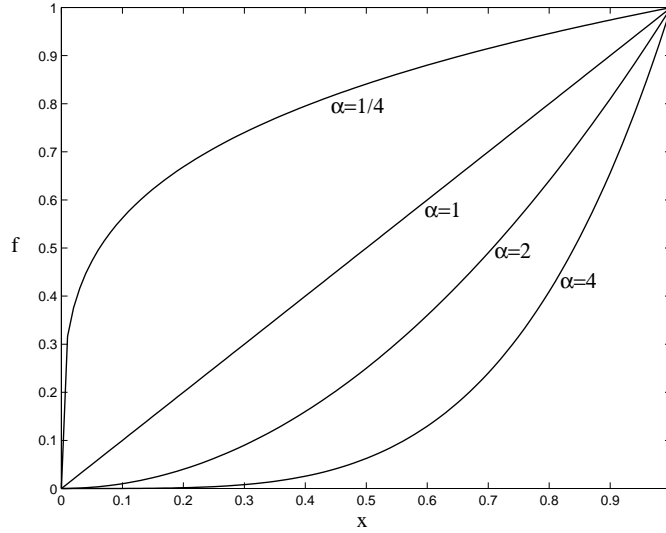
$$(19) \quad y'' + Pf(x)y' - kPyf'(x) = 0,$$

with conditions,

$$(20) \quad y'(0) = 0 \quad \text{and} \quad y(1) = 1 - \frac{y'(1)}{P}.$$

This equation is a homogeneous, linear, second-order differential equation. Both k and P are assumed constant in this application, with the biologically relevant parameter intervals $P \geq 1$ and $0 < k \leq 10$ [10]. Differentiation is taken with respect to x .

In general, $f(x)$ is a monotonically increasing function with $x \in [0, 1]$, ranging between $f(0) = 0$ and $f(1) = 1$. Since the exact form of $f(x)$ is unknown, and a general solution to the equation is not available for arbitrary f , we first solve the

FIGURE 2. Graph of $f = x^\alpha$.

equation for the specific case of $f(x) = x$, whence $f' = 1$. Then we extend these results to include solutions to equation (19) with $f = x^\alpha$ ($\alpha > 0$), which constitute a family of monotonically increasing functions on the interval, encompassing both convex and concave forms. Typical forms of f are illustrated in Figure (2).

4. SOLVING THE MODEL EQUATION

The solution to equation (19) does not present in a simple form, rather in a form involving special functions; in particular, in the form of Kummer functions, a special case of the hypergeometric function. These functions will be defined below where they emerge in the solution.

First we will solve the equation for the particular case of constant transpiration rate across the leaf, $f(x) = x$, using the power series method of solution. This case and method are described in [8], but we outline them here for completeness. We then solve the general case for variable transpiration rate, $f(x) = x^\alpha$, using the confluent hypergeometric equation method of solution.

4.1. Power series method of solution for particular case $f(x) = x$. Set

$$(21) \quad y = \sum_{n=0}^{\infty} a_n x^n,$$

and then we can write equation (19) as

$$(2a_2 - Pka_0) + (6a_3 + Pa_1 - Pka_1)x + (12a_4 + 2Pa_2 - Pka_2)x^2 + \dots = 0.$$

Equating each coefficient of the powers of x to zero we obtain expressions for a_2 , a_3 , a_4 and so on. Substituting these into the series solution (21),

$$\begin{aligned} y &= a_0 + a_1x + \frac{Pka_0}{2}x^2 + \frac{Pa_1(k-1)}{6}x^3 + \frac{Pa_2(k-2)}{12}x^4 + \dots \\ &= a_0 \left(1 + \frac{Pk}{2!}x^2 + \frac{P^2k(k-2)}{2 \times 12}x^4 + \dots \right) + a_1x \left(1 + \frac{P(k-1)}{6}x^2 + \dots \right). \end{aligned}$$

The first condition from equation (20) implies that $a_1 = 0$ and thus the second term is zero.

Applying the transformation $z = -Px^2/2$,

$$(22) \quad y = a_0 \left(1 + \frac{-k}{\frac{1}{2}}z + \frac{-k}{\frac{1}{2}} \frac{(-\frac{k}{2} + 1)}{\frac{3}{2}} \frac{z^2}{2!} + \frac{-k}{\frac{1}{2}} \frac{(-\frac{k}{2} + 1)}{\frac{3}{2}} \frac{(-\frac{k}{2} + 2)}{\frac{5}{2}} \frac{z^3}{3!} + \dots \right)$$

$$= a_0 \Phi \left(-\frac{k}{2}, \frac{1}{2}; z \right).$$

This series is defined as the Kummer series, or confluent hypergeometric series, and in general [1],

$$(23) \quad \Phi(a, b; z) = {}_1F_1(a, b; z) = \sum_{n=0}^{\infty} \frac{a(a+1)(a+2)\dots(a+n-1)}{b(b+1)b+2)\dots(b+n-1)} \frac{z^n}{n!}.$$

The second boundary condition from equation (20) defines a_0 . Following the variable transformation $z = -Px^2/2$, the second condition becomes,

$$y_z(-P/2) = 1 + y'_z(-P/2),$$

where the subscript z implies $y = y(z)$ and differentiation is with respect to z . Thus

$$y_z \left(-\frac{P}{2} \right) = 1 + a_0 \frac{d}{dz} \left[\Phi \left(-\frac{k}{2}, \frac{1}{2}; z \right) \right]_{z=-P/2}$$

$$= 1 + a_0(-k) \Phi \left(1 - \frac{k}{2}, \frac{3}{2}; -\frac{P}{2} \right),$$

where we have used the identity [1],

$$(24) \quad \frac{d}{dz} \Phi(a, b; z) = \frac{a}{b} \Phi(a+1, b+1; z).$$

We can then solve for a_0 , and substituting back into equation (22),

$$(25) \quad y_z = \frac{\Phi \left(-\frac{k}{2}, \frac{1}{2}; z \right)}{\Phi \left(-\frac{k}{2}, \frac{1}{2}; -\frac{P}{2} \right) + k \Phi \left(1 - \frac{k}{2}, \frac{3}{2}; -\frac{P}{2} \right)}.$$

Applying further identities for Kummer functions [1],

$$(26) \quad \Phi(a, b; z) = e^z \Phi(b-a, b; -z),$$

$$(27) \quad 0 = \Phi(a, b-1; z) - \frac{a}{b-1} \Phi(a+1, b; z) + \frac{a-b+1}{b-1} \Phi(a, b; z),$$

with $a = -k/2$ and $b = 3/2$ in the latter, the solution can be written as

$$(28) \quad y_z = \frac{\Phi \left(-\frac{k}{2}, \frac{1}{2}; z \right)}{(1+k) \Phi \left(-\frac{k}{2}, \frac{3}{2}; -\frac{P}{2} \right)} = \frac{e^{\frac{P}{2}+z} \Phi \left(\frac{k}{2} + \frac{1}{2}, \frac{1}{2}; -z \right)}{(1+k) \Phi \left(\frac{k}{2} + \frac{3}{2}, \frac{3}{2}; \frac{P}{2} \right)}.$$

4.2. Confluent hypergeometric form method for general case $f(x) = x^\alpha$. Setting $f(x) = x^\alpha$, and then $f' = \alpha x^{\alpha-1}$, equation (19) becomes

$$(29) \quad y'' + \alpha x^\alpha y' + b x^{\alpha-1} y,$$

where $a = P$ and $b = -kP\alpha$. We apply a transformation which converts our equation into the general confluent hypergeometric form. Let $z = x^{\alpha+1}$, and then equation (29) converts to

$$(\alpha+1)^2 z y''_z + (\alpha+1)(\alpha z + \alpha) y'_z + b y = 0,$$

where the subscript z implies $y = y(z)$ and differentiation is with respect to the new variable z . The hypergeometric function solution to general differential equations of the form

$$(a_2 z + b_2) y'' + (a_1 z + b_1) y' + (a_0 z + b_0) y = 0,$$

is given in [15] as

$$\begin{aligned}
y_z &= C_1 \Phi \left(\frac{b}{a(\alpha+1)}, \frac{\alpha}{\alpha+1}; -\frac{az}{\alpha+1} \right) + C_2 \Psi \left(\frac{b}{a(\alpha+1)}, \frac{\alpha}{\alpha+1}; -\frac{az}{\alpha+1} \right) \\
&= C_1 \Phi \left(\frac{b}{a(\alpha+1)}, \frac{\alpha}{\alpha+1}; -\frac{az}{\alpha+1} \right) \\
&\quad + C_2 \left[\frac{\Gamma \left(1 - \frac{\alpha}{\alpha+1} \right)}{\Gamma \left(\frac{b}{a(\alpha+1)} - \frac{\alpha}{\alpha+1} + 1 \right)} \Phi \left(\frac{b}{a(\alpha+1)}, \frac{\alpha}{\alpha+1}; -\frac{az}{\alpha+1} \right) \right. \\
&\quad \left. + \frac{\Gamma \left(\frac{\alpha}{\alpha+1} - 1 \right)}{\Gamma \left(\frac{b}{a(\alpha+1)} \right)} z^{(1-\frac{\alpha}{\alpha+1})} \Phi \left(\frac{b}{a(\alpha+1)} - \frac{\alpha}{\alpha+1} + 1, 2 - \frac{\alpha}{\alpha+1}; -\frac{az}{\alpha+1} \right) \right] \\
&= C_1 \Phi \left(-\frac{k\alpha}{\alpha+1}, \frac{\alpha}{\alpha+1}; -\frac{Pz}{\alpha+1} \right),
\end{aligned}$$

where C_1 and C_2 are arbitrary constants. The second term of the full solution has coefficient $C_2 = 0$ in order to satisfy the first condition of equation (20).

Constant C_1 can be established from the second boundary condition of equation (20): Since

$$y' = \frac{dy}{dx} = \frac{dy}{dz} \frac{dz}{dx} = y'_z \frac{dz}{dx},$$

then the boundary condition, in terms of the new variable, becomes

$$y(1) = 1 - \frac{y'(1)}{P} \quad \Rightarrow \quad y_z(1) = 1 - y'_z(1) \frac{(\alpha+1)}{P}.$$

Thus, applying identity (24),

$$C_1 \Phi \left(-\frac{k\alpha}{\alpha+1}, \frac{\alpha}{\alpha+1}; -\frac{P}{\alpha+1} \right) = 1 - C_1 k \Phi \left(-\frac{k\alpha}{\alpha+1} + 1, \frac{\alpha}{\alpha+1} + 1; -\frac{P}{\alpha+1} \right),$$

whence we can solve for C_1 and

$$y_z = \frac{\Phi \left(-\frac{k\alpha}{\alpha+1}, \frac{\alpha}{\alpha+1}; -\frac{Pz}{\alpha+1} \right)}{\Phi \left(-\frac{k\alpha}{\alpha+1}, \frac{\alpha}{\alpha+1}; -\frac{P}{\alpha+1} \right) + k \Phi \left(-\frac{k\alpha}{\alpha+1} + 1, \frac{\alpha}{\alpha+1} + 1; -\frac{P}{\alpha+1} \right)}.$$

Applying identities (26) and (27), with $a = -k\alpha/(\alpha+1)$ and $b = 1 + \alpha/(\alpha+1)$ in the latter, this solution can be expressed as

(30)

$$y_z = \frac{\Phi \left(-\frac{k\alpha}{\alpha+1}, \frac{\alpha}{\alpha+1}; -\frac{Pz}{\alpha+1} \right)}{(1+k)\Phi \left(-\frac{k\alpha}{\alpha+1}, \frac{\alpha}{\alpha+1} + 1; -\frac{P}{\alpha+1} \right)} = \frac{e^{\frac{P}{\alpha+1}(1-z)} \Phi \left(\frac{\alpha(k+1)}{\alpha+1}, \frac{\alpha}{\alpha+1}; \frac{Pz}{\alpha+1} \right)}{(1+k)\Phi \left(\frac{\alpha(k+1)}{\alpha+1} + 1, \frac{\alpha}{\alpha+1} + 1; \frac{P}{\alpha+1} \right)}.$$

Note that with $\alpha = 1$ (that is, for $f(x) = x$), and recalling that $z = x^{\alpha+1}$ here, this equation reduces to equation (28) as expected.

5. PROPERTIES OF THE SOLUTION

5.1. Convergence of the series. We show below that, although solution y (equation (30)) is comprised of two infinite series, it converges for all values of the parameters.

A series is convergent if the ratio of the coefficients of two sequential terms in the series approaches zero (see, for example [13]). Using this ratio test, it can be shown that

$$\Phi \left(\frac{\alpha(k+1)}{\alpha+1}, \frac{\alpha}{\alpha+1}; \frac{Px^{\alpha+1}}{\alpha+1} \right)$$

converges for all x , with $x \in [0, 1]$. Consider the ratio of the coefficients of two consecutive terms:

$$\frac{\left(\frac{\alpha(k+1)}{\alpha+1}\right) \left(\frac{\frac{\alpha(k+1)}{\alpha+1}+1}{\frac{\alpha}{\alpha+1}+1}\right) \cdots \left(\frac{\frac{\alpha(k+1)}{\alpha+1}+n}{\frac{\alpha}{\alpha+1}+n}\right) \frac{1}{(n+1)!} \left(\frac{P}{\alpha+1}\right)^{n+1}}{\left(\frac{\alpha(k+1)}{\alpha+1}\right) \left(\frac{\frac{\alpha(k+1)}{\alpha+1}+1}{\frac{\alpha}{\alpha+1}+1}\right) \cdots \left(\frac{\frac{\alpha(k+1)}{\alpha+1}+(n-1)}{\frac{\alpha}{\alpha+1}+(n-1)}\right) \frac{1}{(n)!} \left(\frac{P}{\alpha+1}\right)^n}.$$

Simplifying, and examining the limit as $n \rightarrow \infty$,

$$\lim_{n \rightarrow \infty} \left(\frac{\alpha(k+1) + n(\alpha+1)}{\alpha + n(\alpha+1)} \frac{1}{n+1} \frac{P}{\alpha+1} \right) = 0,$$

since for large n , $[\alpha(k+1) + n(\alpha+1)]/[\alpha + n(\alpha+1)] \rightarrow 1$. Thus the Kummer series above is convergent for all x . (In the same way, it can be established that the Kummer function denominator of equation (30) converges for all k and P .)

5.2. The integral $\int y df$. In order to match the properties of the model with experimental data, it is useful to evaluate the integral of the solution over f .

We can re-arrange equation (19) to give

$$y = \frac{1}{Pk} \left(y'' \frac{dx}{df} + Pfy' \frac{dx}{df} \right).$$

Then

$$\begin{aligned} \int_0^1 y df &= \frac{1}{Pk} \left(\int_0^1 y'' \frac{dx}{df} df + P \int_0^1 fy' \frac{dx}{df} df \right) \\ (31) \qquad &= \frac{1}{Pk} \left(\int_0^1 y'' dx + P \int_0^1 fy' dx \right). \end{aligned}$$

Applying the boundary conditions of equation (20),

$$\int_0^1 y'' dx = y'(1) - y'(0) = (1 - y(1))P,$$

and integrating by parts, it follows that

$$\int_0^1 fy' dx = fy|_0^1 - \int_0^1 y \frac{df}{dx} dx = y(1) - \int_0^1 y df.$$

Substituting back into equation (31),

$$\begin{aligned} \int_0^1 y df &= \frac{1}{Pk} \left[(1 - y(1))P + P \left(y(1) - \int_0^1 y df \right) \right] \\ &= \frac{1}{k} - \frac{y(1)}{k} + \frac{y(1)}{k} - \frac{1}{k} \int_0^1 y df \\ &= \frac{1}{k} - \frac{1}{k} \int_0^1 y df. \end{aligned}$$

Thus

$$(32) \qquad \left(1 + \frac{1}{k} \right) \int_0^1 y df = \frac{1}{k} \quad \Rightarrow \quad \int_0^1 y df = \frac{1}{k+1}.$$

5.3. The integral $\int y dx$. In the special case when $\alpha = 1$ and $f = x$, we have from above

$$(33) \quad \int_0^1 y df = \int_0^1 y dx = \frac{1}{k+1}.$$

However, for $\alpha \neq 1$ this does not hold.

With $f = x^\alpha$, equation (19) becomes

$$y'' + Px^\alpha y' - kP\alpha x^{\alpha-1} y = 0.$$

Thus

$$(34) \quad \begin{aligned} y &= \frac{1}{kP\alpha} x^{1-\alpha} y'' + \frac{1}{k\alpha} xy', \\ \int_0^1 y dx &= \frac{1}{kP\alpha} \int_0^1 x^{1-\alpha} y'' dx + \frac{1}{k\alpha} \int_0^1 xy' dx. \end{aligned}$$

Integrating the first term on the RHS,

$$\int_0^1 x^{1-\alpha} y'' dx = x^{1-\alpha} y'|_0^1 - (1-\alpha) \int_0^1 x^{-\alpha} y' dx = y'(1) + (\alpha-1) \int_0^1 x^{-\alpha} y' dx.$$

and integrating the second term gives

$$\int_0^1 xy' dx = xy|_0^1 - \int_0^1 y dx = y(1) - \int_0^1 y dx.$$

Substituting back into equation (34), and applying the boundary conditions,

$$(35) \quad \begin{aligned} \int_0^1 y dx &= \frac{1}{1+k\alpha} \left[\frac{y'(1)}{P} + y(1) + \frac{(\alpha-1)}{P} \int_0^1 x^{-\alpha} y' dx \right] \\ &= \frac{1}{1+k\alpha} \left[1 + \frac{(\alpha-1)}{P} \int_0^1 x^{-\alpha} y' dx \right]. \end{aligned}$$

Clearly, for $\alpha = 1$ this reduces to $1/(1+k)$ as expected.

Since $y' \geq 0$ on the interval (see below), then

$$\int_0^1 y dx \geq \frac{1}{1+k\alpha} \quad \text{if } \alpha > 1, \quad \text{and} \quad \int_0^1 y dx \leq \frac{1}{1+k\alpha} \quad \text{if } \alpha < 1.$$

In Section 7.2 (to come), we show that when P is large, the solution can be estimated by equation (46), for which the integral is

$$(36) \quad \int_0^1 \frac{P}{P+k\alpha} x^{k\alpha} dx = \left(\frac{P}{P+k\alpha} \right) \left(\frac{1}{1+k\alpha} \right) \approx \frac{1}{1+k\alpha} \quad \text{for } P \gg k\alpha.$$

5.4. The derivative. We can show the solution equation (30) to be monotonically increasing over the interval $[0, 1]$, by examining the derivative.

Let

$$A = -\frac{k\alpha}{\alpha+1}, \quad B = \frac{\alpha}{\alpha+1} \quad \text{and} \quad z = x^{\alpha+1},$$

so that, from identities (24) and (26),

$$(37) \quad \begin{aligned} y &= \frac{e^{\frac{P}{\alpha+1}(1-z)}}{k+1} \frac{\Phi\left(B-A, B; \frac{Pz}{\alpha+1}\right)}{\Phi\left(B-A+1, B+1; \frac{P}{\alpha+1}\right)}, \\ y' &= \frac{e^{\frac{P}{\alpha+1}(1-z)} P x^\alpha}{k+1} \left[\frac{\frac{B-A}{B} \Phi\left(B-A+1, B+1; \frac{Pz}{\alpha+1}\right) - \Phi\left(B-A, B; \frac{Pz}{\alpha+1}\right)}{\Phi\left(B-A+1, B+1; \frac{P}{\alpha+1}\right)} \right]. \end{aligned}$$

Note that α , P and k are positive, and $x \in [0, 1]$. Now, since $0 \leq B \leq (B - A)$, then $(B - A + n)/(B + n) \geq 1$ for all positive integers n . Expanding the numerator within the square brackets of y' above, it follows from the definition of Kummer functions that $y' \geq 0$.

Note, from the second condition of equation (20), $y'(0) = 0$, so that the solution curve is either constant, or concave upwards through $x = 0$ with $y''(0) \geq 0$ there.

6. RELATING OUR SOLUTION AND ITS PROPERTIES TO THE BIOLOGY

In order to relate our results to the biology, we use solution y to establish the isotopic enrichments in the xylem, at the sites of evaporation, in the lamina mesophyll and in the veinlets which link the xylem to the lamina mesophyll, relative to source water: that is, Δ_x , Δ_e , Δ_{rl} and Δ_{rv} , respectively. We then establish expressions for the average of each of these, across the whole leaf, and discuss their significance.

6.1. Isotopic enrichment of the xylem, lamina and evaporation sites. From our definition of y , in the first paragraph of Section 3, we have $y = (\Delta_M - \Delta_x)/\Delta_M$ where $\Delta_x = R_x/R_s - 1$ is the oxygen isotopic composition in xylem water, and $\Delta_M = R_M/R_s - 1$ is the maximum such composition. (Recall that R_s is the isotopic ratio of source water entering the leaf base, and R_M is the maximum possible ratio in leaf water.) By definition,

$$(38) \quad \frac{\Delta_x}{\Delta_M} = 1 - y \quad \Rightarrow \quad \Delta_x = \Delta_M (1 - y).$$

Given the maximum possible enrichment, relative to source water, this expression applies our solution to describe the enrichment of the xylem water Δ_x .

We can also establish an expression for the isotopic composition at the sites of evaporation. From equations (14) and (9), and with the usual definition of Δ ($\Delta_E = R_E/R_s - 1$ for transpired water, and $\Delta_e = R_e/R_s - 1$ at the sites of transpiration),

$$(39) \quad \Delta_E = \frac{e^{P_r} \Delta_x - h' \Delta_M}{e^{P_r} - h'}, \quad \text{and} \quad \Delta_e = \Delta_E + (\Delta_x - \Delta_E) e^{P_r}.$$

In order to establish the average enrichment in the lamina mesophyll (Δ_{rl}), we note that water travels from the xylem to the lamina along veinlets. Although the mass contribution from the water in these veinlets is negligible, compared with that of the xylem and lamina, they may account for a significant difference in enrichment between the xylem and lamina. We include this concept in our model by considering the enrichment in each component, the veinlets and the lamina, separately.

For the veinlets the average value of R (the isotope ratio at a location r from the xylem) over the range of the veinlet, from $r = 0$ to $r = r_v$, can be found by integrating equation (8):

$$(40) \quad \begin{aligned} R_{rv} &= \frac{1}{r_v} \int_0^{r_v} R dr = R_E - (R_x - R_E) \frac{e^{P_{rv}} - 1}{P_{rv}}, \\ \Rightarrow \Delta_{rv} &= \Delta_E + (\Delta_x - \Delta_E) \frac{e^{P_{rv}} - 1}{P_{rv}}, \end{aligned}$$

where $P_{rv} = v_r r_v / D$ is the Péclet number associated with fluxes in the veinlets.

In the mesophyll we calculate the average of R from $r = r_v$ to $r = r_e$:

$$\begin{aligned} R_{rl} &= \frac{1}{r_e - r_v} \int_{r_v}^{r_e} R dr = R_E - (R_x - R_E) \frac{e^{P_r} - e^{P_{rv}}}{P_r - P_{rv}}, \\ \Rightarrow \Delta_{rl} &= \Delta_E + (\Delta_x - \Delta_E) \frac{e^{P_r} - e^{P_{rv}}}{P_r - P_{rv}}, \\ (41) \quad &= \Delta_E + (\Delta_x - \Delta_E) e^{P_r} \frac{1 - e^{-P_{rl}}}{P_{rl}}, \end{aligned}$$

where $P_{rl} = P_r - P_{rv} = v_r(r_e - r_v)/D$ is the Péclet number associated with fluxes in the lamina.

Note that, comparing equations (39) and (41), for $P_{rl} > 0$ we have $\Delta_e > \Delta_{rl}$ (since $(1 - e^{-P_{rl}})/P_{rl} < 1$), implying that enrichment near the sites of evaporation is greater than that in the lamina.

Thus equations (38), (39), (40) and (41) establish the isotopic enrichment in the xylem, at the sites of transpiration, in the veinlets and in the lamina mesophyll, respectively, in terms of the solution y (equation (30)) to the differential equation model (19). (Methods for calculating or estimating y are described in Section 7.) These equations hold, regardless of whether E (the rate of transpiration) varies across the leaf or not. Variation, due to variation in transpiration rates, enters through α in solution (30).

6.2. Average isotopic enrichment of the xylem, lamina and evaporation sites, over the whole leaf. Using the above results, we can now establish spatial average enrichments, taken over the whole leaf, for the components.

We consider first the average enrichment of xylem water, and make use of the integral established in Section 5.2, equations (33) and (36):

$$\bar{\Delta}_x = \int_0^1 \Delta_x dx = \begin{cases} \Delta_M \left(1 - \frac{1}{1+\alpha k}\right) & \text{if } \alpha \neq 1 \text{ and } P \text{ large,} \\ \Delta_M \left(1 - \frac{1}{1+k}\right) & \text{if } \alpha = 1, \end{cases}$$

where the equality is approximate for $\alpha \neq 1$. Since $k = h'/(e^{P_r} - h')$ (equation (14)),

$$(42) \quad \bar{\Delta}_x = \begin{cases} \approx h' \Delta_M \frac{\alpha}{e^{P_r} + h'(\alpha-1)} & \text{if } \alpha \neq 1 \text{ and } P \text{ large,} \\ h' \Delta_M \frac{1}{e^{P_r}} & \text{if } \alpha = 1. \end{cases}$$

This provides an expression for the average (over a whole leaf) isotopic enrichment of the xylem water, relative to source water, for the cases of constant or variable transpiration rates.

For the average enrichment of transpired water we have, from equations (39) and (42),

$$(43) \quad \bar{\Delta}_E = \frac{e^{P_r} \bar{\Delta}_x - h' \Delta_M}{e^{P_r} - h'} = \begin{cases} \approx h' \Delta_M \frac{\alpha-1}{e^{P_r} + h'(\alpha-1)} & \text{if } \alpha \neq 1 \text{ and } P \text{ large,} \\ 0 & \text{if } \alpha = 1. \end{cases}$$

Note that,

$$\bar{\Delta}_E \approx h' \Delta_M \frac{1}{\frac{e^{P_r}}{\alpha-1} + h'},$$

which is approximately zero when α is close to 1. From equation (43), there is no enrichment of transpired water relative to source water in the case of constant transpiration, as expected. In the case of variable transpiration rate, the transpiration weighted average gives the same result (see equation (32)). However, although the measurement of total transpired water from a leaf will have no enrichment with respect to source water, the average, as calculated above with respect to length, need not be zero.

Further, from equations (39) and (42), it follows that the average enrichment over all sites of evaporation is

$$\bar{\Delta}_e = \bar{\Delta}_E + (\bar{\Delta}_x - \bar{\Delta}_E)e^{P_r} = \begin{cases} \approx h' \Delta_M \frac{\alpha - 1 + e^{P_r}}{e^{P_r} + h'(\alpha - 1)} & \text{if } \alpha \neq 1 \text{ and } P \text{ large,} \\ h' \Delta_M & \text{if } \alpha = 1. \end{cases}$$

Similarly, the average enrichments for all veinlets and over the whole lamina mesophyll follow from equations (40) and (41), together with results (42) and (43) above. They are, respectively,

$$\begin{aligned} \bar{\Delta}_{rv} &= \begin{cases} \approx h' \Delta_M \frac{1}{e^{P_r} + h'(\alpha - 1)} \left(\alpha - 1 + \frac{e^{P_{rv}} - 1}{P_{rv}} \right) & \text{if } \alpha \neq 1 \text{ and } P \text{ large,} \\ h' \Delta_M \frac{1}{e^{P_r}} \frac{e^{P_{rv}} - 1}{P_{rv}} & \text{if } \alpha = 1, \end{cases} \\ \bar{\Delta}_{rl} &= \begin{cases} \approx h' \Delta_M \frac{1}{e^{P_r} + h'(\alpha - 1)} \left(\alpha - 1 + e^{P_r} \frac{1 - e^{-P_{rl}}}{P_{rl}} \right) & \text{if } \alpha \neq 1 \text{ and } P \text{ large,} \\ h' \Delta_M \frac{1 - e^{-P_{rl}}}{P_{rl}} & \text{if } \alpha = 1. \end{cases} \end{aligned} \quad (44)$$

Note that, for $P_{rl} > 0$ (since $(1 - e^{-P_{rl}})/P_{rl} < 1$) we have $\bar{\Delta}_e > \bar{\Delta}_{rl}$, indicating that the average enrichment is greatest close to the transpiration sites.

The significance of establishing the isotopic enrichment in the lamina is that it translates to organic matter, which can be measured. It is in this mesophyll water where sucrose is synthesised, and if the Péclet number is known then humidity and temperature can be established, which in turn facilitate climate reconstruction.

7. CALCULATING OR ESTIMATING MODEL SOLUTION y

Solution y , equation (30), to model equation (19) is not straightforward to calculate. Below, we discuss methods of calculating or estimating the solution.

7.1. Mathematical software packages. A mathematical software package can be used, for example the symbolic packages of Mathematica and Maple, to evaluate the Kummer function solutions for fixed parameter values.

For Maple, solution (28) can be calculated by setting the parameter values, as well as a particular z value, and using the command

$$[> \text{evalf} \left(\text{KummerM} \left(\frac{k}{2} + \frac{1}{2}, \frac{1}{2}, z \right) \right);$$

To plot the solution over an interval, apply the command

$$[> \text{with}(plots) : \text{plot} \left(\text{KummerM} \left(\frac{k}{2} + \frac{1}{2}, \frac{1}{2}, \frac{Px^2}{2} \right), x = 0..1 \right);$$

The equivalent commands to calculate the Kummer function in Mathematica are,

$$\text{Hypergeometric1F1} \left[\frac{k}{2} + \frac{1}{2}, \frac{1}{2}, z \right]$$

although the plotting of this function is complex.

However, such packages are not always available, and some alternative methods for estimating the solution are suggested below. Such estimates may also reveal simple behaviour, ‘hidden’ in the Kummer function

7.2. Estimating the solution analytically. There are a number of conditions under which a solution can be found, which provide a very good estimate of the full solution (28) or (30). They are simpler to evaluate than the full Kummer function solution.

7.2.1. *Case of large P .* When P is large, $P \gg 10$, the differential equation (19) can be approximated by

$$(45) \quad x^\alpha y' = kx^{\alpha-1}y.$$

This is a separable, first-order differential equation, with solution

$$y = Ax^{k\alpha},$$

where A is the arbitrary constant emerging through integration. Applying the second boundary condition of equation (20) to solve for A ,

$$(46) \quad y \approx \frac{P}{P + k\alpha} x^{k\alpha}.$$

When $k\alpha \ll P$, then $y \approx x^{k\alpha}$.

In particular, when $\alpha = 1$ and $f = x$, then $y \approx (Px^k/(P+k))$ and $y \approx x^k$ when $k \ll P$.

It should be noted here that, although this function is a good approximation across most of the $[0, 1]$ interval, it does not approximate well close to $x = 0$, unless $P \geq 10^3$ when the y -intercept approaches zero. And it is the behaviour of the solution in this very region (for $x \ll 1$) that is of most interest for the biology, as in this region a characteristic ‘flattening’ is observed in the collected data. (See Section 9 to come.)

7.2.2. *Special cases which are simple to evaluate.* For certain values of k (regardless of P) the Kummer function simplifies and thus the solution becomes easy to calculate.

In some cases, many terms of the Kummer function evaluate to zero. Consider the Kummer function numerator of solution (30):

$$\begin{aligned} \Phi \left(-\frac{k\alpha}{\alpha+1}, \frac{\alpha}{\alpha+1}; -\frac{Pz}{\alpha+1} \right) = \\ 1 + (-k) \frac{-Px^{\alpha+1}}{\alpha+1} + \frac{(-k)}{1} \frac{(-k\alpha + (\alpha+1))}{(2\alpha+1)} \left(\frac{-Px^{\alpha+1}}{\alpha+1} \right)^2 \frac{1}{2!} + \\ \frac{(-k)}{1} \frac{(-k\alpha + (\alpha+1))}{(2\alpha+1)} \frac{(-k\alpha + 2(\alpha+1))}{(3\alpha+2)} \left(\frac{-Px^{\alpha+1}}{\alpha+1} \right)^3 \frac{1}{3!} \dots \end{aligned}$$

Clearly, when $k = 0$, all terms after the first drop out, and the full solution (30) is $y = 1$. In general, if $k = n(\alpha+1)/\alpha$ for some natural number n , then all terms after, and including, the $(n+2)^{\text{th}}$ term are zero.

In particular, when $\alpha = 1$, $f = x$ and k is even, the solutions are simple to evaluate. From solution (28)

$$\begin{aligned} k = 2 \quad \Rightarrow \quad y &= \frac{1 + Px^2}{(1+P)(k+1)}, \\ k = 4 \quad \Rightarrow \quad y &= \frac{1 + 2Px^2 + \frac{1}{3}P^2x^4}{(1 + 2P + \frac{1}{3}P^2)(k+1)}, \end{aligned}$$

and so on.

7.2.3. *An estimate for y .* In Section 5, we established the solution to be convergent, and from the result $y' \geq 0$ we have that on the interval $[0, 1]$ the solution is increasing, with a minimum at $x = 0$. Directly from solution equation (30), the y -intercept decreases from 1 to 0, as parameters P or k are increased. Above, we have discussed the case for P large, as well as the case when k is an integer multiple of $(\alpha+1)/\alpha$. When P is small, and $k \neq n(\alpha+1)/\alpha$, we require some other means for estimating the solution.

One method, is to calculate the first few terms of the full solution, equation (28) or (30), since $x \leq 1$ and the series is convergent. In particular,

$$(47) \quad y \approx a_0 + a_1 x^{\alpha+1} + a_2 (x^{\alpha+1})^2$$

is a reasonable estimate, where the coefficients are taken from the series expansion and are thus

$$(48) \quad \begin{aligned} a_0 &= \frac{1}{(k+1)\Phi\left(\frac{-k\alpha}{\alpha+1}, \frac{\alpha}{\alpha+1} + 1; \frac{-P}{\alpha+1}\right)}, \\ a_1 &= a_0 \left(-\frac{P}{\alpha+1}(-k)\right), \\ a_2 &= a_0 \left(\left(-\frac{P}{\alpha+1}\right)^2 \frac{(-k)}{1} \frac{(-k\alpha + \alpha + 1)}{2\alpha + 1} \frac{1}{2!}\right). \end{aligned}$$

This estimate yields good results while equation (47) is increasing on the interval $[0, 1]$.

More generally, a reasonable estimate for y is given by a combination of equations (46) and (47) (the latter being particularly accurate for x close to 0). From inspection, and for the parameter intervals $0 < k \leq 1$ and $1 \leq P \leq 100$,

$$\begin{aligned} y &\approx a_0 + a_1 x^{\alpha+1} + a_2 (x^{\alpha+1})^2 && \text{if } x_c \geq 1, \\ y &\approx \left\{ \begin{array}{ll} a_0 + a_1 x^{\alpha+1} + a_2 (x^{\alpha+1})^2 & \text{while } x < x_c \\ \frac{P}{P+k\alpha} x^{k\alpha} & \text{while } x \geq x_c \end{array} \right\} && \text{if } 0 < x_c < 1, \\ y &\approx \frac{P}{P+k\alpha} x^{k\alpha} && \text{if } x_c \text{ is imaginary,} \end{aligned}$$

where x_c is the positive inflection point of equation (47). Taking the second derivative of (47) and equating it to zero gives,

$$x_c = \left(\frac{n(n+1)}{P(n+1-kn)} \right)^{\frac{1}{n+1}}.$$

Further, for $Pk > 500$, equation (46) is a good estimate.

For the purposes of calculation, and for the particular cases when $\alpha = 1/2, 1$ and 2 , the values for a_0 (the y -intercept) can be read from the graphs in Figure (3).

7.3. Graphs of the solution with changing parameters. Finally, some graphs are included to illustrate how the solution equation (30) behaves, and how it changes with parameter variation.

Figures (4) and (5) are for the case when $\alpha = 1$, and parameters P and k allowed to vary. In general, increases in P and/or k serve to reduce the y -intercept with $y(0) \rightarrow 0$. Increases in P increase the value of $y(1)$, and $y(1) \rightarrow 1$. In contrast, increases in k reduce the value of $y(1)$.

Figure (6) illustrates changes in the solution with variations in α . In general, for $\alpha \leq 1$, the solutions (equation (30)) lie above one another, with the uppermost being that for the least value of α . Thus decreasing $\alpha < 1$ serves to increase both $y(0)$ as well as $y(1)$. Increasing $\alpha > 1$, has the impact of reducing $y(1)$, with the lowest value of $y(1)$ corresponding to the largest α .

8. MODEL MODIFICATION FOR TAPERING XYLEM

In the above formulation, the xylem was modelled with a cylinder of constant cross sectional area a_x along its length. We now relax this assumption, allowing the xylem to taper, and examine how this impacts on our model.

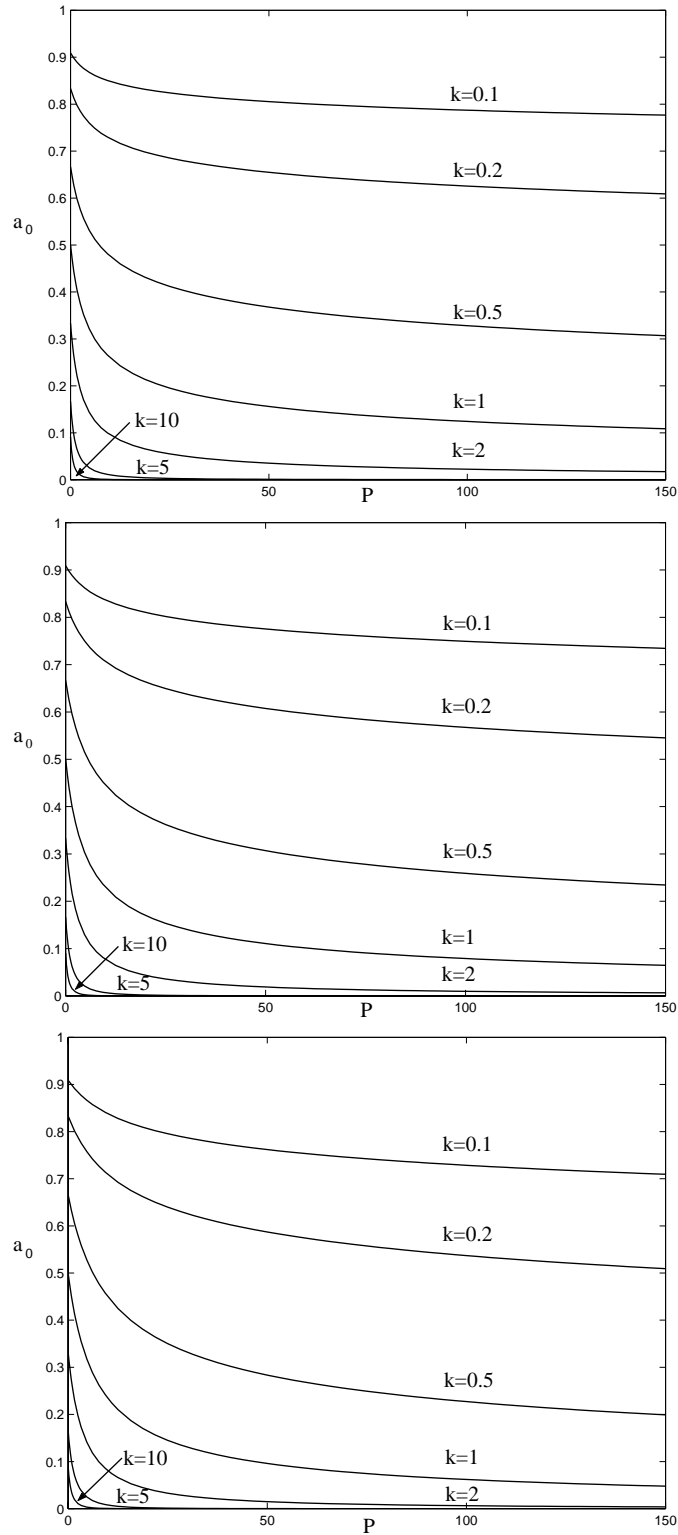


FIGURE 3. Graphs of a_0 (equation (48)) for the cases, from the uppermost, of $\alpha = 1/2$, $\alpha = 1$ and $\alpha = 2$.

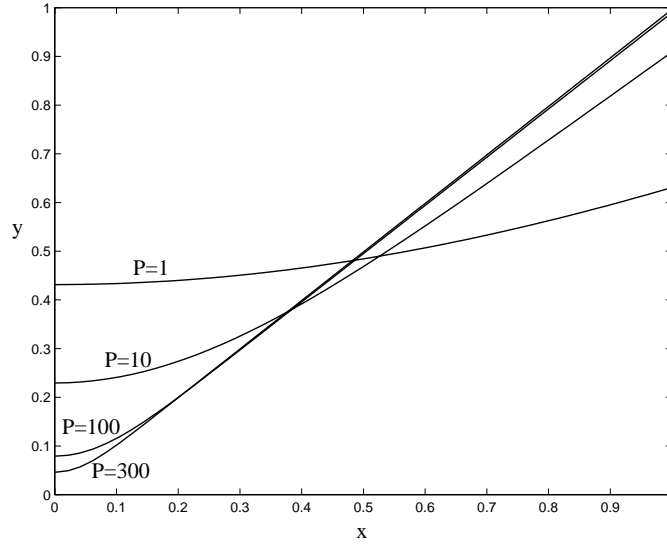


FIGURE 4. Solution equation (28), with $k = 1$ fixed, and P varying from $P = 1$, through $P = 10$, $P = 100$ and $P = 300$.

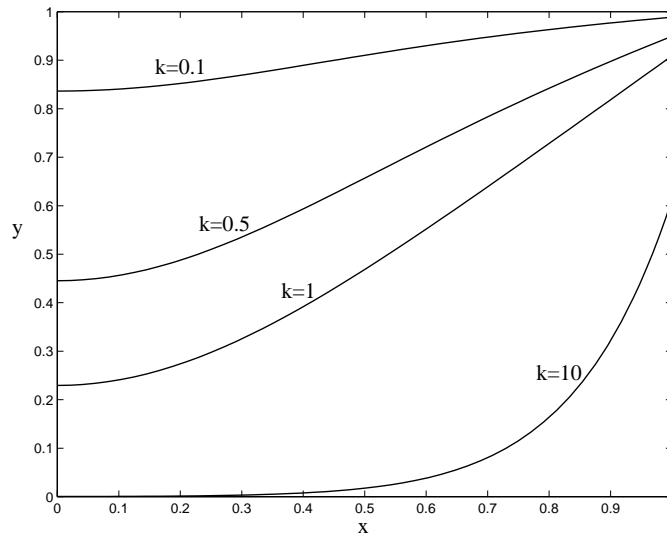


FIGURE 5. Solution equation (28), with $P = 10$ fixed, and k varying from $k = 0.1$, through $k = 0.5$, $k = 1$ and $k = 10$.

8.1. Model formulation. With reference to our initial formulation, the total mass flux through advection is balanced by the loss through transpiration, so that equation (2) is unchanged. However, inclusion of a tapering xylem introduces a further term in equation (3), since a_x is no longer constant. Equation (3) becomes

$$Cva_x \frac{dR_x}{dl} + R_x \frac{d(Cva_x)}{dl} = a_x D \frac{d^2(R_x C)}{dl^2} + D \frac{d(R_x C)}{dl} \frac{da_x}{dl} - R_E E_s,$$

whence equation (6), with tapering, is

$$(49) \quad a_x DC \frac{d^2 R_x}{dl^2} - (I_m - I) \frac{dR_x}{dl} + (R_x - R_E) \frac{dI}{dl} = -DC \frac{dR_x}{dl} \frac{da_x}{dl}.$$

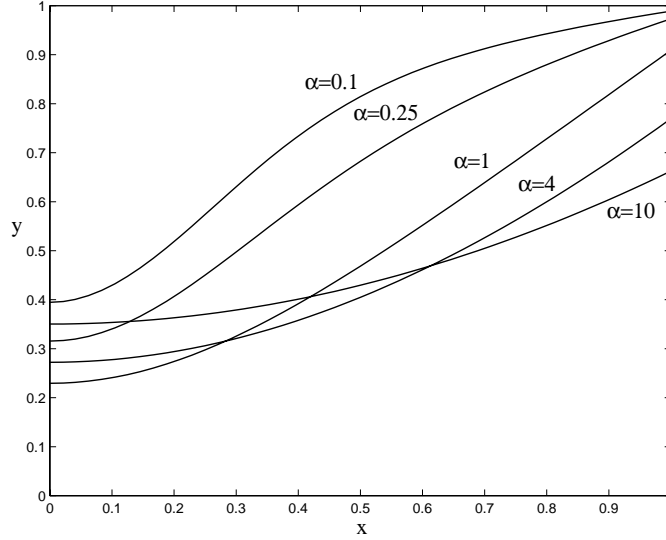


FIGURE 6. Solution equation (30), with $k = 1$ and $P = 10$ fixed, and $f = x^\alpha$ with values for α given on each graph.

When a_x is constant with length, the RHS equates to zero as expected. When $a_x = a_x(l)$ then the equation includes contributions from both the advective and diffusive fluxes, which depend on the taper of the xylem, da_x/dl . The diffusive contribution is explicit (appearing on the RHS of the equation above), whereas the advective contribution presents implicitly through the variables $I(l)$ and $E(l)$.

Including transport and diffusion between the xylem and lamina mesophyll follows in the same manner as for the case of constant xylem cross-sectional area, and thus equation (49) transforms to

$$(50) \quad a_x DC \frac{d^2 R_x}{dl^2} - \left[(I_m - I) - DC \frac{da_x}{dl} \right] \frac{dR_x}{dl} + k(R_M - R_x) \frac{dI}{dl} = 0.$$

8.2. Boundary conditions. The boundary conditions in this case for tapering xylem, are identical to those where the xylem cross sectional area was assumed constant. Thus at the leaf tip equation (17) holds, while at the base of the leaf there are no changes to the condition (18).

8.3. Scaling the equation. First we make some assumptions about the manner in which the xylem tapers. We assume the tapering to be approximately linear ([2] and [3]), and that the cross-sectional area at the tip ($l = l_m$) is $\hat{\gamma}$ times the cross-sectional area at the base ($l = 0$). Then

$$a_x(l) = a_x(0) - \frac{(a_x(0) - \hat{\gamma} a_x(0))}{l_m} l = a_x(0) \left(1 - \gamma \frac{l}{l_m} \right),$$

where $\gamma = 1 - \hat{\gamma}$. Following the same process as in Section 3, and including a linear taper, we can transform equation (50) to non-dimensional form:

$$\begin{aligned}
 0 &= a_x(0) \left(1 - \gamma \frac{l}{l_m}\right) DC \frac{d^2 R_x}{dl^2} - \left[(I_m - I) - DC \frac{-a_x(0)\gamma}{l_m} \right] \frac{dR_x}{dl} \\
 &\quad + k(R_M - R_x) \frac{dI}{dl} \\
 &= \frac{a_x(0)DC}{I_m l_m^2} \left(1 - \gamma \frac{l}{l_m}\right) \frac{d^2 R_x}{d(l/l_m)^2} \\
 &\quad - \left[\left(1 - \frac{I}{I_m}\right) + \frac{a_x(0)\gamma DC}{I_m l_m} \right] \frac{1}{l_m} \frac{dR_x}{d(l/l_m)} + \frac{k}{l_m} (R_M - R_x) \frac{d(I/I_m)}{d(l/l_m)} \\
 &= \frac{a_x(0)v_0 C}{I_m} \frac{D}{v_0 l_m^2} \left(1 - \gamma \frac{l}{l_m}\right) \frac{d^2 R_x}{d(l/l_m)^2} \\
 &\quad - \left[\left(1 - \frac{I}{I_m}\right) + \frac{a_x(0)v_0 C}{I_m} \frac{D}{v_0 l_m} \gamma \right] \frac{1}{l_m} \frac{dR_x}{d(l/l_m)} + \frac{k}{l_m} (R_M - R_x) \frac{d(I/I_m)}{d(l/l_m)},
 \end{aligned}$$

where v_0 is the velocity of water at the leaf base. Now, setting

$$f = 1 - \frac{I}{I_m}, \quad x = 1 - \frac{l}{l_m}, \quad y = 1 - \frac{\Delta_x}{\Delta_M}, \quad \text{and} \quad \frac{1}{P} = \frac{D}{v_0 l_m},$$

and noting that $a_x(0)v_0 C = I_m$, we have

$$\begin{aligned}
 0 &= \frac{1 - \gamma(1 - x)}{P} \frac{d^2 R_x}{dx^2} + \left(f + \frac{\gamma}{P}\right) \frac{dR_x}{dx} + k(R_M - R_x) \frac{df}{dx} \\
 (51) \quad \Rightarrow 0 &= \frac{(1 - \gamma + \gamma x)}{P} \frac{d^2 y}{dx^2} + \left(f + \frac{\gamma}{P}\right) \frac{dy}{dx} - ky \frac{df}{dx}.
 \end{aligned}$$

For $\gamma = 0$ (no taper) this equation simplifies to the case of constant a_x , equation (19), as expected.

8.4. Model solution. The authors were unable to obtain a ‘nice’ analytical form for a general solution to equation (51); however, a number of numerical simulations were performed in order to compare these solutions which include xylem taper, with those for the case of cylindrical xylem. The results are presented in Figure 7.

In the special case when $\alpha = 1$ a solution can be obtained for variable γ , by applying the same methods as in Section 4:

$$\begin{aligned}
 y &= \frac{\Phi\left(-k, 1 - \frac{P(1-\gamma)}{\gamma^2}; -\frac{Px}{\gamma} - \frac{P(1-\gamma)}{\gamma^2}\right)}{\Phi\left(-k, 1 - \frac{P(1-\gamma)}{\gamma^2}; -\frac{Px}{\gamma}\right) + \frac{k\gamma}{\gamma^2 - P(1-\gamma)} \Phi\left(-k + 1, 2 - \frac{P(1-\gamma)}{\gamma^2}; -\frac{Px}{\gamma}\right)} \\
 \rightarrow &\frac{\Phi(-k, 1; -Px)}{(1+k)\Phi(-k, 2; -P)} = e^{P-Px} \frac{\Phi(k+1, 1; Px)}{(1+k)\Phi(k+2, 2; P)} \quad \text{as } \gamma \rightarrow 1.
 \end{aligned}$$

9. COMPARING THE MODEL OUTPUT WITH BIOLOGICAL DATA

We now examine to what extent the model developed predicts the features seen in the data, where we will use, as an example for comparison, data collected by Kim Suan Gan for maize leaves [10],[11]. Such leaves have long (550-900 mm), minimally branched and approximately parallel veins, some of which extend for the full length of the leaf blade, while others, towards the outer edges of the blade, terminate earlier. Each vein, of which there are typically eight on each side of the mid-vein, is comprised of, on average, three xylem vessels. Such a configuration facilitates reasonable estimates for the relevant Péclet numbers required for our model application, and, while it is recognised that this model remains a simplification of the mechanisms operating within maize leaves, this configuration is well suited to our model.

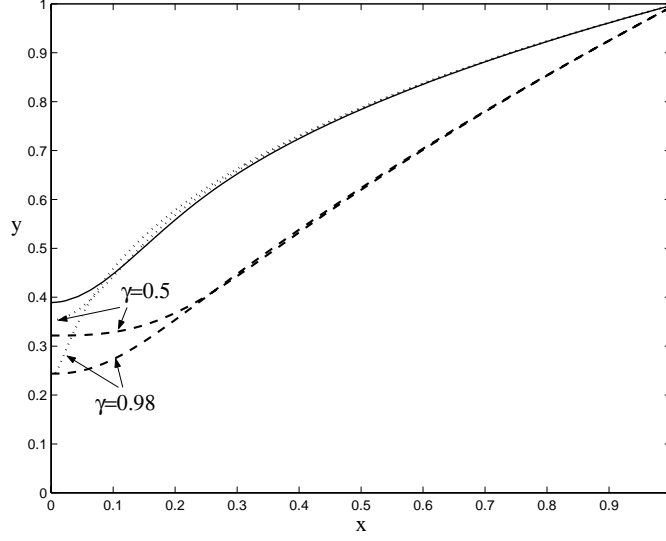


FIGURE 7. The case of no taper and $\alpha = 1$ is given by the solid line. The dotted lines represent two cases of tapering with $\alpha = 1$, and the dashed curves represent two cases of tapering with $\alpha = 2$. (Parameters $P = 100$ and $k = 0.341$ are fixed. These values were chosen to provide a comparison with the data of Section 9.)

Progressive enrichment of water, in both the xylem and lamina mesophyll, was observed along the length of the leaf blade, varying with both distance along the blade and proximity to the mid-vein, as well as with relative humidity. Enrichment in the veins increased towards the leaf tip (with a maximum at the tip), as well as increasing with distance from the mid-vein towards the edges of the leaf. Although these features were retained with varying humidity, the magnitude of the changes along the vein, and outwards from the mid-vein, was much greater under low humidity conditions, with the enrichment rising more steeply near the leaf tip. (For full details of the measuring process and results, see [11].)

We need to establish measured and modelled quantities which can be compared. Leaf water in segments of leaf is comprised of contributions from the veins and lamina, as well as the veinlets between them. Collected data measurements are of this total leaf water; thus, relative to source water, Δ_{lw} is measured, and Δ_{lw}/Δ_M can be calculated. In order to establish the same quantity from our model output, we relate the total leaf water in a segment to the relative contributions from the veins and lamina. For the case of constant or variable transpiration across the leaf,

$$(52) \quad \frac{\Delta_{lw}}{\Delta_M} = \rho_1 \frac{\Delta_x}{\Delta_M} + \rho_2 \frac{\Delta_{rv}}{\Delta_M} + \rho_3 \frac{\Delta_{rl}}{\Delta_M} \approx \rho_1 \frac{\Delta_x}{\Delta_M} + (1 - \rho_1) \frac{\Delta_{rl}}{\Delta_M},$$

where $\rho_1 + \rho_2 + \rho_3 = 1$, and each represent the water fraction associated with veins, veinlets and lamina mesophyll, respectively. ρ_1 is estimated as 0.43 for maize [10], while $\rho_2 \approx 0$ since the mass contribution from the veinlets is negligible compared with that of the lamina. Thus $\rho_3 \approx (1 - \rho_1) = 0.57$. The RHS can be calculated from our model output through equations (38) and (41), and solution (30).

Further, since our model predicts the enrichment close to, and along, a single vein, we need to adapt this formulation to the leaf configuration. In a typical maize leaf there are eight such veins on either side of the mid-vein, with the outermost terminating at a distance of $0.6l_m$ along the blade. Thus we model the system by summing the contributions from each vein, for which the lengths are taken to

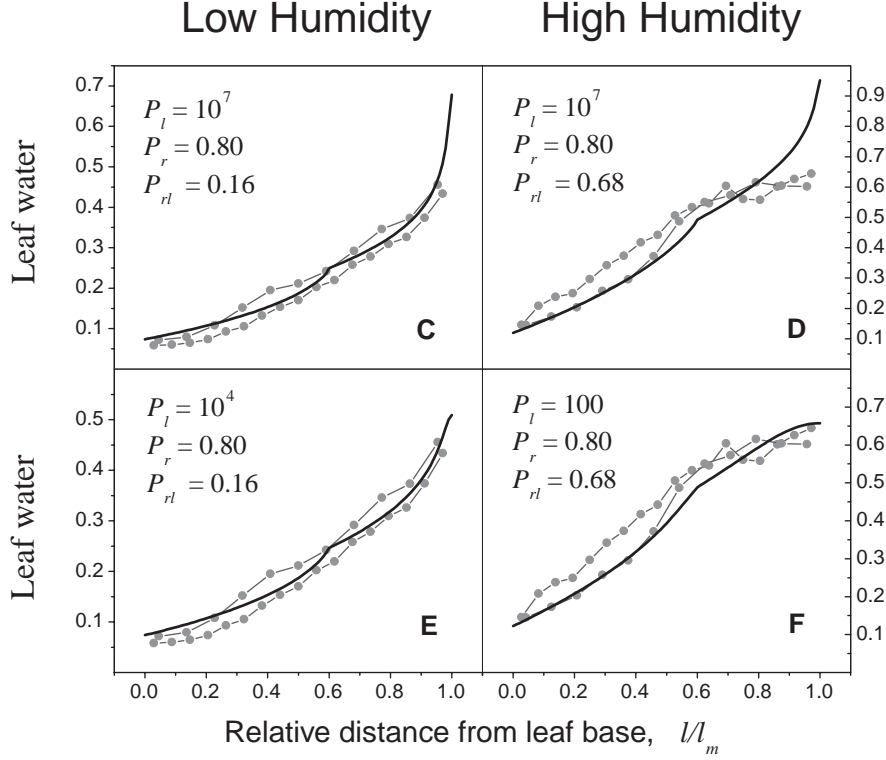


FIGURE 8. Leaf water Δ_{lw}/Δ_M is plotted from the model output (solid line) and from collected data (joined dots), for the case of constant transpiration rate across the leaf surface, that is, $f = x$. The plots on the LHS are for low humidity conditions with $k = 0.125$, while those on the RHS are for high humidity with $k = 0.341$. The Péclet numbers (with $P = P_l$) are as on the plots.

become progressively longer towards the mid-vein (from $0.6l_m$ to l_m), and smooth the curves.

Parameters used in the model predictions are as follows. The Péclet number associated with longitudinal fluxes in the xylem was calculated from measurements in the mid-vein: $P \approx 10^7$ [10]. This estimate was independent of humidity. Since advection and diffusion in this longitudinal direction also occur in the lamina, and this effect has not been included in the model, the above estimate of P is expected to be a substantial overestimate for the leaf as a whole: thus we assume a better estimate of P to be $P \approx 10^4$. The Péclet number associated with flux between the xylem and lamina was estimated as $P_r \approx 0.8$, comprising contributions from the lamina mesophyll $P_{rl} < 2.5$ and the veinlets joining the xylem to the lamina $P_{rv} < 0.75$ [10]. This leads to an approximation of parameter k from its definition after equation (14). Parameter values for h' are measured quantities established at data collection, with $h' = 0.243$ for low humidity conditions, and $h' = 0.566$ for high humidity.

Comparisons between the model output (solid lines) and data measurements (joined dots) are presented in Figures 8 and 9. The model output is calculated from equation (52) (where $\rho_1 = 0.43$), with Δ_x , Δ_E and Δ_{rl} from equations (38),

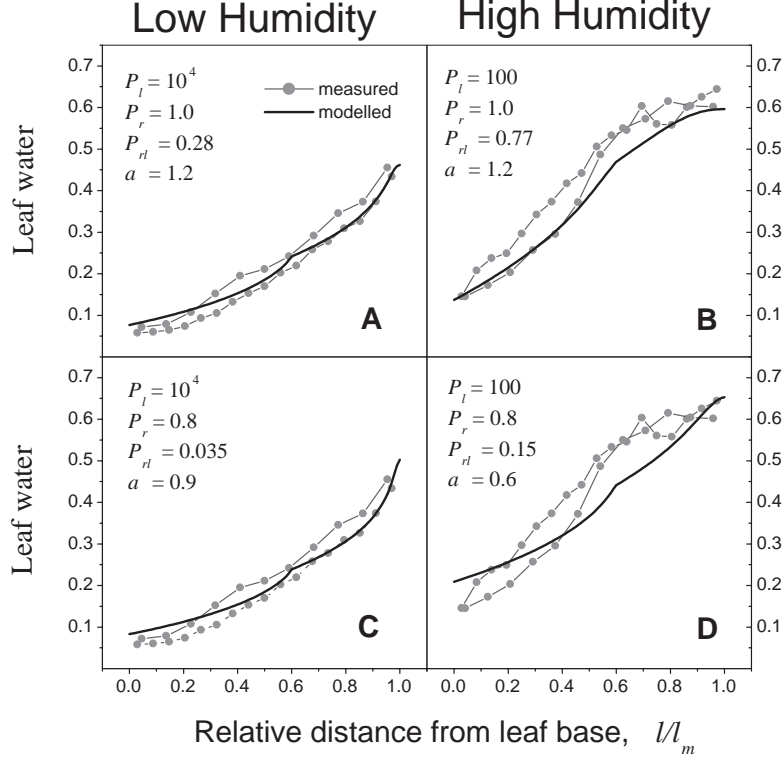


FIGURE 9. Leaf water Δ_{lw}/Δ_M is plotted from the model output (solid line) and from collected data (joined dots), for the case of variable transpiration rate across the leaf surface, that is, $f = x^\alpha$. The plots on the LHS are for low humidity conditions with $k = 0.098$ for $P_r = 1$ and $k = 0.125$ for $P_r = 0.8$, while those on the RHS are for high humidity with $k = 0.263$ for $P_r = 1$ and $k = 0.341$ for $P_r = 0.8$. The Péclet numbers (with $P = P_l$) and values for α are as on the plots.

(39) and (41), respectively, solution y from (30) and parameter values as given in the captions.

For Figure 8, $f = x$ is assumed, implying a constant transpiration rate across the leaf. Note that, for high humidity, smaller values of the longitudinal Péclet number provide a better fit to the data, while for low humidity this sensitivity is reduced. In general, this was found to be the case suggesting values for P to be overestimated under high humidity conditions.

Figure 9 introduces the effect of varying transpiration rate, with $f = x^\alpha$ and $\alpha \neq 1$. For low humidity, the inclusion of a variable transpiration rate does not improve the fit markedly. However, in the case of high humidity, the agreement between the model and data is significantly increased with $\alpha = 1.2$. A further improvement is achieved by adjusting the Péclet numbers P_{rv} and P_{rl} , as illustrated in Figure 10. Such a variation remains well within the error margin associated with the measurements and estimation of these Péclet numbers.

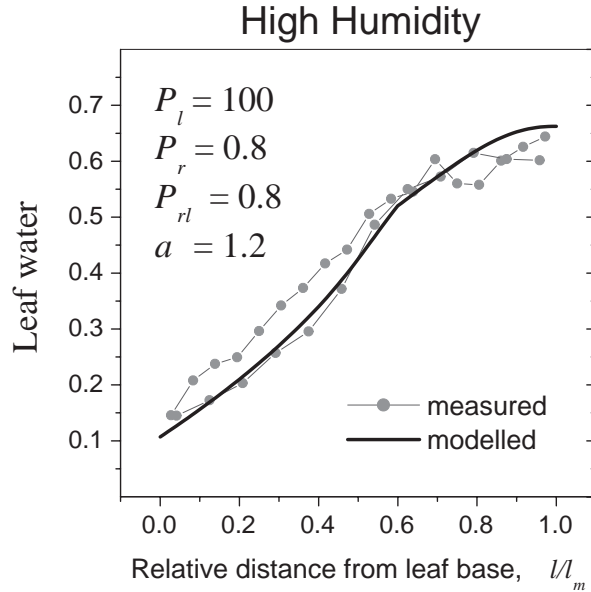


FIGURE 10. Leaf water Δ_{lw}/Δ_M is plotted from the model output (solid line) and from collected data (joined dots), for the case of variable transpiration rate across the leaf surface, that is, $f = x^\alpha$. The plot illustrates the best fit in the case of high humidity with $k = 0.341$. The Péclet numbers (with $P = P_l$) and value for α are as on the plot.

10. CONCLUSIONS

We have presented a full formulation and mathematical analysis of the Farquhar-Gan model, as proposed in [8]. In this paper, the model has been extended to include the more general case when transpiration rates may vary across the leaf surface, and where veins taper with length. The model solutions take the form of special functions, and thus we have presented certain relevant properties of the solutions, and some means of estimating them from simpler functions. Collected data do not necessarily feed directly into the model parameters, so we have established the means by which these solutions, and their properties, can be compared with measurements.

Although the model remains a simplification of the transport processes of heavy isotopes within the leaf, in general it predicts the main and subtle observed features of leaf water enrichment. Lower values of the originally estimated Péclet number P provide a better fit to the measured data, and, as discussed in Section 9, this overestimate may result from the exclusion of longitudinal diffusion along the length of the leaf in the lamina mesophyll. Further, in the case of high humidity, the extension of the model presented in this paper to include variable transpiration across the leaf surface, improves the agreement between model predictions and the observations.

In spite of the close match between model and measurements, there remain shortcomings in the formulation which require further work. The study highlights the need for data on transpiration rates and the nature of its variability across the leaf surface, in order to establish a ‘true’ functional form for f in our model. Also,

as noted in the text, R_x is given as the ratio of abundances, $\text{H}_2^{18}\text{O}/\text{H}_2^{16}\text{O}$, and thus our model remains an approximation, reliant upon the small relative abundance of H_2^{18}O molecules in leaf water.

REFERENCES

- [1] M. Abramowitz and I. A. Stegun. *Handbook of Mathematical Functions*. National Bureau of Standards, Washington D. C., 1965.
- [2] D. Altus and M. Canny. Water pathways in wheat leaves. i. the division of fluxes between different vein types. *Australian Journal of Plant Physiology*, 12:173–181, 1985.
- [3] D. Altus, M. Canny, and D. Blackman. Water pathways in wheat leaves. ii. water-conducting capacities and vessel diameters of different vein types, and the behaviour of the integrated vein network. *Australian Journal of Plant Physiology*, 12:183–199, 1985.
- [4] H. Craig and L. Gordon. Deuterium and oxygen-18 variations in the ocean and marine atmosphere. In E. Tongiorgi, editor, *Proceedings of a conference on Stable Isotopes in Oceanographic Studies and Paleotemperatures*, pages 9–130. CNR, Laboratorie Geologia Nuclear, Pisa, Italy, 1965.
- [5] G. Dongmann, H. Nürnberg, H. Förstel, and K. Wagener. On the enrichment of H_2^{18}O in the leaves of transpiring plants. *Radiation and Environmental Biophysics*, 11:41–52, 1974.
- [6] G. Farquhar, J. Lloyd, J. Taylor, Flanagan L, Syvertsen J, K. Hubick, S. Wong, and J. Ehleringer. Vegetation effects on the isotope composition on oxygen in atmospheric CO_2 . *Nature*, 363:439–443, 1993.
- [7] G. Farquhar and J. Lloyd. Carbon and oxygen isotope effects on the exchange of carbon dioxide between terrestrial plants and the atmosphere. In J. Ehleringer, A. Hall, and G. Farquhar, editors, *Stable Isotopes and PLant Carbon-Water Relations*, pages 47–70. Academic Press, New York, 1993.
- [8] Graham Farquhar and Kim Suan Gan. On the progressive enrichment of the oxygen isotopic composition of water along a leaf. *PLant, Cell and Environment (in press)*, 2002.
- [9] F. Leaney, C. Osmond, G. Allison, and H. Zeigler. Hydrogen-isotope composition of leaf water in C_3 and C_4 plants: its relationship to the hydrogen-isotope composition of dry matter. *Planta*, 164:215–220, 1985.
- [10] Kim Suan Gan. *Oxygen Isotope Ratio of Leaf Water*. PhD Thesis, Canberra, 2002.
- [11] Kim Suan Gan, Suan Chin Wong, Jean Wan Hong Yong, and Graham D. Farquhar. Evaluation of models of leaf water ^{18}O enrichment using measurements of spatial patterns of vein xylem, leaf water and dry matter in maize leaves. *Plant Cell and Environment (submitted)*, 2002.
- [12] J. Gat and C. Bowser. The heavy isotope enrichment of water in coupled evaporative systems. In H. Taylor, J. O’Neil, and I. Kaplan, editors, *Stable Isotope Geochemistry: A tribute to Samuel Epstein*, pages 159–168. The Geochemical Society, Lancaster Press, St. Louis, 1991.
- [13] E. Kreyszig. *Advanced Engineering Mathematics*. John Wiley and Sons, New York, sixth edition, 1988.
- [14] R. Mills and K. Harris. The effect of isotopic substitution on diffusion in liquids. *Chemical Society Reviews*, 5(2), 1976.
- [15] A. D. Polyanin and V. F. Zaitsev. *Handbook of Exact Solutions for Ordinary Differential Equations*. CRC Press, New York, 1995.

[†]RESEARCH SCHOOL OF BIOLOGICAL SCIENCES, AUSTRALIAN NATIONAL UNIVERSITY, CANBERRA, ACT 0200, AUSTRALIA.